Published by IOP Publishing for SISSA
Received: *September 4, 2008*
Accepted: *October 12, 2008*
Published: *October 14, 2008*

A new world sheet field theory*

Korkut Bardakci

University of California at Berkeley, University of California, Berkeley, California 94720, U.S.A., and
Theoretical Physics Group, Lawrence Berkeley National Laboratory, University of California, Berkeley, California 94720, U.S.A.
E-mail: kbardakci@lbl.gov

Abstract: A second quantized field theory on the world sheet is developed for summing planar graphs of the ϕ^3 theory. This is in contrast to the earlier work, which was based on first quantization. The ground state of the model is investigated with the help of a variational ansatz. In complete agreement with standard perturbation theory, the infinities encountered in carrying out this calculation can be eliminated by the renormalization of the parameters of the model. We also find that, as in the earlier work, in the ground state, graphs form a dense network (condensate) on the world sheet.

Keywords: Nonperturbative Effects, 1/N Expansion.

*This work was supported by the Director, Office of Science, Office of High Energy Physics, of the U.S. Department of Energy under Contract DE-AC02-05CH11231.

JHEP10(2008)056

Contents

1. Introduction

This paper is the continuation of a series of papers devoted to the summation of field theory graphs on the world sheet [1 – 4], but at the same time, it is a fresh start. As in the previous work, the starting point is 't Hooft's seminal paper [5], which puts planar Feynman graphs of the ϕ^3 field theory on the world sheet parametrized by the light cone variables. The world sheet is again discretized , and extensive use is made of the fermions introduced in [6] to ennumerate graphs. But other than these features, the present article differs substantially from the earlier work on the same problem.

All the previous papers on this subject, starting with [1], used the formalism of first quantization: The momenta flowing through the graph were treated as fields and quantized. This approach was inspired by the well known quantization of free strings on the world sheet, and in fact, the idea behind the two parallel treatments was to build a bridge between field theoery and string theory. In contrast, the present article is based on a second quantized Fock space approach, very much along the lines suggested in 't Hooft's original paper [5]. As explained in section 2, on the world sheet, a typical graph of the ϕ^3 theory can be pictured as a collection of parallel solid lines, which form the boundaries of the propagators (see figure 1). The idea is to define fields ϕ and $\phi^\dagger$ (eq. (3.1)), which annihilate and create these lines, and construct the corresponding Fock space. This is analogous to the usual second quantization of field theory, where the corresponding field operators create and annihilate particles. Here, the analogue of particles are the points on the solid lines that mark the boundaries of the propagators. From this perspective, $\phi^\dagger$ and ϕ create and annihilate boundaries.

The Fock space construction outlined above has one serious defect: It has infinitely many unwanted states. They correspond to multiple solid lines at the same location, and

also to unallowed configuration of propagators. In section 3, making crucial use of the world sheet fermions [6], we show how to overcome this problem. Consequently, in addition to the ϕ's, the Fock space must also include the fermions. In sections 3 and 4, we construct the free and the interacting Hamiltonians in terms of these operators. The corresponding time development operator is then shown to generate all all the planar graphs of ϕ^3 on the world sheet.

At this point, one can pose a natural question: What is the motivation for inventing a new formalism for summing planar graphs? We list a couple responses to this question:

a) It is always a good idea to to try to find many different approaches to a difficult problem, with their different advantages and disadvantages.

b) In our opinion, the new formalism is both simpler than the previous one, and also it is better founded. The difficulties encountered in the old formalism were discussed extensively in reference [4]; we will not repeat this discussion here except to note that they all arose from technical issues connected with first quantization. In contrast, the new approach based on second quantization is both simple and encounters no such problems. As an added bonus, in contrast to the old approach, it is easy to introduce a finite mass.

c) In section 5, we study the ground state of the system, using a variational approximation scheme. In this calculation, we encounter ultraviolet divergences, which have to be renormalized. In the critical dimension of space-time, which is six for the ϕ^3 theory, the divergences are the standard ones familiar from perturbation theory; namely, logarithmic divergence in the coupling constant and quadratic divergence in the mass. The model can be renormalized in the usual fashion by absorbing these divergences into the bare parameters. Also, the well known asymptotic freedom of the theory comes out of the variational calculation. This is all very satisfactory, especially compared to the earlier work, where renormalization of the model was always a problem.

Of course, the idea behind the whole program is not just to reproduce some results of perturbation theory but to go beyond them. The variational calculation was mainly set up to compute the parameter ρ_0, defined by eqs. (2.5) and (5.2). This parameter measures the density of the solid lines (boundaries) on the world sheet, which will be defined precisely at the beginning of section 5. Any finite order graph consists of a finite number of solid lines, which form a set of zero density on the world sheet. Therefore, the corresponding ρ_0 vanishes. A non-zero value for this parameter means that the world sheet is densely occupied by the graphs, and the contribution of high (infinite) order graphs dominate the ground state. Another and perhaps more familiar way is to think of ρ_0 as an order parameter for phase transition. A non-vanishing value for it signals the formation of a new non-perturbative phase corresponding to a densely occupied world sheet. In fact, the variational calculation carried out in section 5 gives a non-zero value for ρ_0, showing that the model is in this new phase.

JHEP10(2008)056

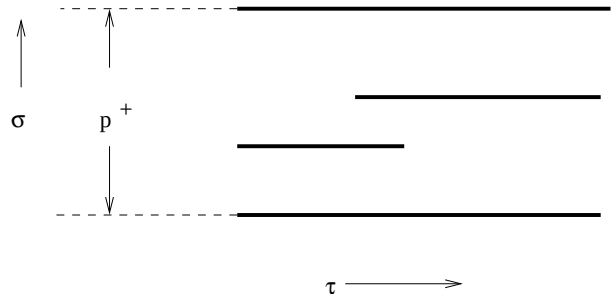

Figure 1: A Typical Graph

In ending this section, we would like to stress that the reformulation of planar ϕ^3 as a world sheet field theory was the crucial first step. Without such a formulation, we would not know how to define the concept of the density of Feynman graphs, let alone introduce an order parameter for a new phase. The simple variational ansatz of eq. (5.3) also relies heavily on the world sheet picture.

2. A brief review

The generic[1] planar graphs of ϕ^3 theory in the mixed light cone representation of 't Hooft [5] have a particularly simple form, which we briefly review here. The world sheet is parametrized by the two coordinates

$$\tau = x^+ = (x^0 + x^1)/\sqrt{2}, \;\; \sigma = p^+ = (p^0 + p^1)/\sqrt{2}.$$

A general planar graph is represented by a collection of horizontal solid lines (figure 1), where the n'th solid line carries a D dimensional transverse momentum $\mathbf{q}_n$. Two adjacent lines labeled by n and n+1 represent the light cone propagator

$$\Delta(p_n) = \frac{\theta(\tau)}{2p^+} \exp\left(-i\tau \, \frac{\mathbf{p}_n^2 + m^2}{2p^+}\right), \tag{2.1}$$

where $\mathbf{p}_n = \mathbf{q}_n - \mathbf{q}_{n+1}$. A factor of g, the coupling constant, is inserted at the beginning and at the end of each line, where the interaction takes place.

For various technical reasons, it is very convenient to discretize the coordinate σ in steps of length a, which is equivalent to compactifying the light cone coordinate $x^- = (x^0 - x^1)/\sqrt{2}$ at radius $R = 1/a$. This type of compactification was first introduced in connection with the M theory [7, 8]; it can be viewed as an infinite boost of the more standard compactification of a spacelike direction. In this paper, we will exclusively work with the discretized world sheet; on the other hand, the time coordinate τ will remain continuous.

We also have to specify the boundary conditions to be imposed on the world sheet. For simplicity, the coordinate σ is compactified by imposing periodic boundary conditions at

[1] By generic, we mean a graph where the external momenta do not have any symmetry pattern. For a discussion, see [4].

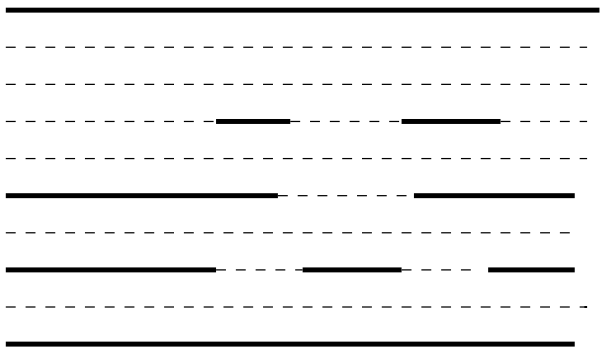

Figure 2: Solid And Dotted Lines

$\sigma = 0$ and $\sigma = p^+$, where p^+ is the total + component of the momentum flowing through the whole graph. In contrast, the boundary conditions at $\tau = \pm\infty$ will be left free; in the Hamiltonian approach that we are going to adopt, they will not play any role.

There is a useful way of visualizing the discretized world sheet, pictured in figure 2. In this picture, the world sheet consists of horizontal dotted and solid lines, spaced a distance a apart. The boundaries of the propagators are marked by solid lines, same as in figure 1, and the bulk is filled with dotted lines. Ultimately, one has to integrate over all possible locations and lengths of solid lines, as well as over the transverse momenta they carry. The integrations over the locations of the solid lines can be conveniently incorporated into the action or the Hamiltonian formalism by introducing a two component fermion field $\psi_i(\sigma,\tau), i = 1, 2$, and its adjoint $\bar{\psi}_i$ [6]. These fields satisfy the usual anticommutation relations

$$\left[\psi_i(\sigma,\tau), \bar{\psi}_{i'}(\sigma',\tau)\right]_+ = \delta_{i,i'}\,\delta_{\sigma,\sigma'}. \tag{2.2}$$

The fermion with $i = 1$ lives on the dotted lines and the one with $i = 2$ lives on the solid lines. On an uninterrupted line, they satisfy the time evolution equation

$$\partial_\tau \psi_i = 0,\ \partial_\tau \bar{\psi}_i = 0. \tag{2.3}$$

On the other hand, when the interaction takes place, there is a transition from $i = 1$ to $i = 2$ or vice versa. The operators that generate these transitions are given by[2]

$$\rho_\pm = \bar{\psi}\sigma_\pm\psi, \tag{2.4}$$

where

$$\sigma_\pm = (\sigma_1 \pm \sigma_2)/2.$$

For future use, we also note that, the operator

$$\rho = \frac{1}{2}\,\bar{\psi}(1 - \sigma_3)\psi, \tag{2.5}$$

is equal to one on the solid lines and zero on the dotted lines.

[2]Here we are using the letter σ for both the world sheet coordinate and also for Pauli matrices. Hopefully, there should be no confusion about the dual use of this letter.

JHEP10(2008)056

3. The free hamiltonian

We start by defining the Hilbert space, which should completely specify the σ cross section of any given graph at a fixed value of the time τ . At each site, labeled by a discrete value of σ, there is either a dotted or a solid line, and a single fermion is placed at that site with $i = 1$ (spin up) in case of a dotted line, and with $i = 2$ (spin down) in case of a solid line. For a solid line, one has also to specify the momentum $\mathbf{q}$ flowing through it, and for this purpose, we introduce the bosonic field $\phi(\sigma, \tau, \mathbf{q})$, and its conjugate $\phi^\dagger(\sigma, \tau, \mathbf{q})$, which at time τ respectively annihilate and create a solid line carrying momentum $\mathbf{q}$ located at site labeled by σ. They satisfy the commutation relations

$$\Big[\phi(\sigma, \tau, \mathbf{q}), \phi^\dagger(\sigma', \tau, \mathbf{q}')\Big] = \delta_{\sigma,\sigma'}\, \delta(\mathbf{q} - \mathbf{q}'). \tag{3.1}$$

We now have both the fermionic and bosonic operators needed to construct the Fock space, and it remains to define the vacuum state. This corresponds to a state with only dotted lines (an empty world sheet), and it satisfies,

$$\rho_+(\sigma)|0\rangle = 0, \;\; \phi(\sigma, \mathbf{q})|0\rangle = 0. \tag{3.2}$$

These conditions are initially imposed at a fixed time τ for all values of σ and $\mathbf{q}$. In equations of this type, we usually do not explicitly write the dependence on time. Of course, the equations of motion ensure that these conditions are satisfied for all times.

It is now easy to construct the Fock space in the standard way. For example, the state corresponding to two solid lines (a propagator) located at σ_1 and σ_2, carrying momenta $\mathbf{q}_1$ and $\mathbf{q}_2$, is given by,

$$|1, 2\rangle = \Big(\phi^\dagger(\sigma_1, \mathbf{q}_1)\, \rho_-(\sigma_1)\Big)\, \Big(\phi^\dagger(\sigma_2, \mathbf{q}_2)\, \rho_-(\sigma_2)\Big)\, |0\rangle. \tag{3.3}$$

Notice that, to preserve the relation between the solid and the dotted lines and the fermion spin (index i), the field ϕ is always accompanied by the field ρ_+ at the same point, and the field $\phi^\dagger$ by ρ_- at the same point.

At this point, it might appear that the introduction of the fermions was redundant. After all, we could have tried to construct the Fock space using only the operators ϕ and $\phi^\dagger$. However, the construction without the fermions runs into a serious problem. In the Hilbert space without the fermions, there will be states corresponding to multiple solid lines at the same site, created by the repeated application of $\phi^\dagger$ at the same σ. For example, the state

$$\prod_{k=1}^{k=n} \phi^\dagger(\sigma, \mathbf{q}_k)|0\rangle$$

corresponds an n-tuple solid line at site σ, which has no world sheet counterpart. This multiple line clearly carries a momentum

$$\sum_{k=1}^{k=n} \mathbf{q}_k,$$

but since already there is a single line carrying the same momentum, the existence of multiple solid lines leads to an infinite overcounting of the states. At this point, the fermions come to the rescue. Because of Fermi statistics

$$(\rho_-(\sigma))^n = 0 \tag{3.4}$$

for $n \geq 2$. Since we associate each $\phi^\dagger$ with a factor of ρ_- at the same site, states corresponding to multiple lines automatically vanish.

The absence of multiple lines (solid or dotted) can be written in the form of an equation of constraint to be imposed on the Hilbert space. We define the operator

$$n(\sigma,\tau) = \int d\mathbf{q}\, \phi^\dagger(\sigma,\tau,\mathbf{q})\, \phi(\sigma,\tau,\mathbf{q}), \tag{3.5}$$

which counts the number of solid lines located at σ. We also recall that the operator $\rho(\sigma,\tau)$, defined earlier (eq. (2.5)), is one if there is a solid line at σ, zero otherwise. It follows that, imposing the constraint

$$\rho(\sigma,\tau) - n(\sigma,\tau) = 0, \tag{3.6}$$

eliminates multiple lines. This constraint is first imposed at a fixed τ for all σ, and in order to extend it to all τ, we have to show that it commutes with the Hamiltonian. We will do so once we have the Hamiltonian at hand.

With these preliminaries out of the way, we turn to the construction of the Hamiltonian for the free theory, where both the solid and dotted lines are eternal, and the graphs are just a collection of free propagators. Consider the state corresponding to a single propagator defined by eq. (3.3). If we tentatively set,

$$H_0 = \frac{1}{2} \sum_{\sigma'>\sigma} \int d\mathbf{q} \int d\mathbf{q}'\, \frac{(\mathbf{q}-\mathbf{q}')^2 + m^2}{\sigma'-\sigma}\, \phi^\dagger(\sigma,\mathbf{q})\, \phi(\sigma,\mathbf{q})\, \phi^\dagger(\sigma',\mathbf{q}')\, \phi(\sigma',\mathbf{q}'), \tag{3.7}$$

it easy to show that

$$H_0|1,2\rangle = \int d\mathbf{q}_1 \int d\mathbf{q}_2\, \frac{(\mathbf{q}_1-\mathbf{q}_2)^2 + m^2}{2\,|\sigma_1-\sigma_2|}. \tag{3.8}$$

The time evolution operator

$$\exp\left(-i\tau H_0\right)$$

then reproduces the free propagator of eq. (2.1), except for the prefactor $1/(2p^+)$. This missing factor will later be included in the interaction Hamiltonian.

Although our proposal for the free Hamiltonian gives the right answer for a single propagator, it does not work in the case of more than one propagator. For example, consider two propagators, whose boundaries are located at σ_1, σ_2 and σ_3, as shown in figure 3. If we apply the free Hamiltonian given by eq. (3.7) to the state corresponding to this figure, in addition to the two propagators with momenta $\mathbf{q}_1 - \mathbf{q}_2$ and $\mathbf{q}_2 - \mathbf{q}_3$, we also get a third unwanted propagator with momentum $\mathbf{q}_1 - \mathbf{q}_3$. The rule is that the propagators are associated with adjacent solid lines such as $1, 2$ and $2, 3$, and not with non-adjacent

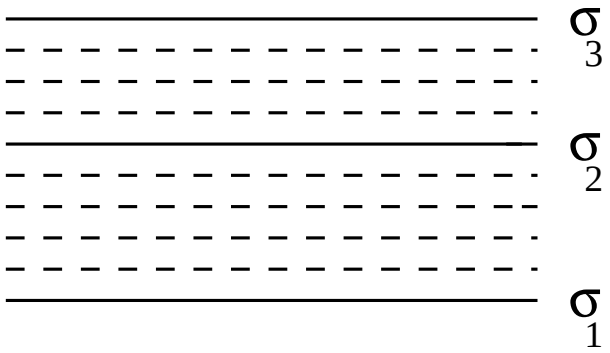

Figure 3: Two Propagators

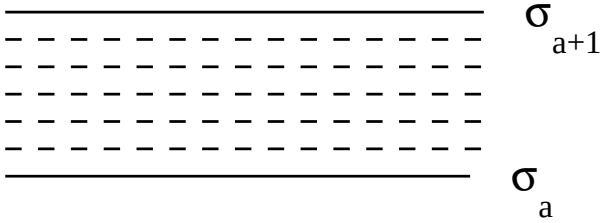

Figure 4: Solid Lines Seperated By Only Dotted Lines

ones, such as $1, 3$. To implement this rule automatically in the expression for H_0, we define, for any two lines, solid or dotted, located at σ_i and σ_j, with $\sigma_j > \sigma_i$,

$$\mathcal{E}(\sigma_i, \sigma_j) = \prod_{k=i+1}^{k=j-1} (1 - \rho(\sigma_k)) \,, \tag{3.9}$$

where ρ is given by eq. (2.5). If $\sigma_j < \sigma_i$, $\mathcal{E}$ is defined to be zero.[3] From its definition, $\mathcal{E}(\sigma_i, \sigma_j)$ is equal to one only if two solid lines are located at σ_i and σ_j, seperated by only dotted lines, as in figure 4. Otherwise, it is zero. In the example discussed above, $\mathcal{E}(\sigma_i, \sigma_j)$ is one for the combinations $i = 1, j = 2$ and $i = 2, j = 3$, and it vanishes for the unwanted combination $i = 1, j = 3$. With the help of this operator, we write the correct version of eq. (3.7):

$$\begin{aligned} H_0 = \frac{1}{2} \sum_{\sigma,\sigma'} \int d\mathbf{q} \int d\mathbf{q}' \, \frac{\mathcal{E}(\sigma, \sigma')}{\sigma' - \sigma} \left((\mathbf{q} - \mathbf{q}')^2 + m^2 \right) \\ \times \, \phi^\dagger(\sigma, \mathbf{q}) \, \phi(\sigma, \mathbf{q}) \, \phi^\dagger(\sigma', \mathbf{q}') \, \phi(\sigma', \mathbf{q}'). \end{aligned} \tag{3.10}$$

By applying H_0 to a state with several solid lines, one can easily show that there is no longer the problem of unwanted propagators. We note the fermions play a dual role: In addition to preventing the formation of multiple solid lines, they eliminate the unwanted configurations of the propagators.

[3] A similar function was introduced for the same reason in [4].

Finally, by making use of the canonical algebra (eq. (3.1)), and the commutation relation

$$\big[\rho(\sigma,\tau),\rho(\sigma',\tau)\big]=0,$$

one can verify that

$$[(\rho-n),H_0]=0. \tag{3.11}$$

This shows that the constraint imposed on the states by eq. (3.6) is consistent with the time evolution.

4. The interaction

The interaction takes place at the point of transition between a solid and a dotted line. These transitions can be generated by the interaction Hamiltonian composed of two terms,

$$H_I=g\sum_\sigma\int d\mathbf{q}\left(\rho_+(\sigma)\,\phi(\sigma,\mathbf{q})+\phi^\dagger(\sigma,\mathbf{q})\,\rho_-(\sigma)\right), \tag{4.1}$$

one of which converts a dotted line into a solid one and the other does the opposite. Also notice that, in accordance with the rule stated after eq. (3.3), $\phi^\dagger$ is accompanied by a factor of ρ_- and ϕ by ρ_+. Then, using the commutation relations

$$\big[\rho(\sigma),\rho_\pm(\sigma')\big]=\mp\,\delta_{\sigma,\sigma'}\,\rho_\pm(\sigma),$$

it is easy to verify that

$$[(\rho-n),H_I]=0. \tag{4.2}$$

This takes care of the interaction, but as we have explained earlier, there are still the missing $1/(2p^+)$ prefactors of the propagators that have to be incorporated into the interaction vertices. Consider the two types of vertices, corresponding to the beginning and ending of a solid line, pictured in figure 5. The solid lines are labeled as 1, 2 and 3, and the momenta that enter the vertex are labeled by the corresponding pair of indices 12, 23, and 13 respectively. As explained in reference [4], attaching a factor of

$$V=\frac{1}{\sqrt{8\,p^+_{12}\,p^+_{23}\,p^+_{13}}}=\frac{1}{\sqrt{8(\sigma_2-\sigma_1)(\sigma_3-\sigma_2)(\sigma_3-\sigma_1)}} \tag{4.3}$$

to each vertex, takes care of the missing prefactors.

We face, however, the following problem: How do we attach V to H_I? It is clear that we should identify σ_2 with the interaction point σ in eq. (4.1), but what about $\sigma_{1,3}$? We have to remember that H_I acts on a state with solid lines located at some sites labeled, say, by σ_a. The sites labeled by σ_1 and σ_3 in figure 5a must then coincide with the two adjacent solid lines labeled by σ_a and σ_{a+1} for some a. To enforce this constraint, we attach a projection operator $\mathcal{F}(\sigma_1,\sigma_3)$ to V. This operator is one when σ_1 and σ_3 are located on two adjacent solid lines of the state, that is, when they are seperated by only dotted

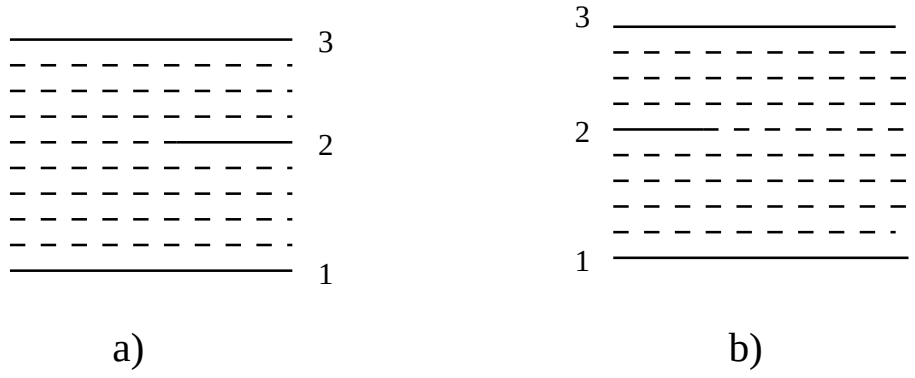

Figure 5: The Two ϕ^3 Vertices

lines. Otherwise, it vanishes. We already faced a similar problem in constructing the free Hamiltonian, and we define a projection operator closely related to $\mathcal{E}$ (eq. (3.9)):[4]

$$\mathcal{F}(\sigma_1, \sigma_3) = \rho(\sigma_1)\, \mathcal{E}(\sigma_1, \sigma_3)\, \rho(\sigma_3), \tag{4.4}$$

and with the help of $\mathcal{F}$, we construct the vertex

$$\mathcal{V}(\sigma_2) = \sum_{\sigma_1<\sigma_2} \sum_{\sigma_3>\sigma_2} \frac{\mathcal{F}(\sigma_1, \sigma_3)}{\sqrt{8\,(\sigma_2-\sigma_1)\,(\sigma_3-\sigma_2)\,(\sigma_3-\sigma_1)}}. \tag{4.5}$$

It is then easy to see that the projection operator lines up σ_1 and σ_3 correctly with the adjacent solid lines of the state on which it acts. This vertex has to be attached to H_I of eq. (4.1) to supply the missing $1/(2p^+)$ factors. With this modification, the final form of the interaction Hamiltonian is,

$$H_I = g \sum_\sigma \int d\mathbf{q} \left(\rho_+(\sigma)\, \phi(\sigma, \mathbf{q})\, \mathcal{V}(\sigma) + \mathcal{V}(\sigma)\, \phi^\dagger(\sigma, \mathbf{q})\, \rho_-(\sigma) \right), \tag{4.6}$$

and the full Hamiltonian is given by,

$$H = H_0 + H_I. \tag{4.7}$$

The above Hamiltonian, combined with the constraint (3.6), generates all the planar graphs on the world sheet.

Although we will stick with the Hamiltonian approach in this paper, if so desired, one can easily switch to the path integral approach based on the action

$$S = \int d\tau \left(\sum_\sigma \left(i\bar{\psi}\partial_\tau \psi + i \int d\mathbf{q}\, \phi^\dagger \partial_\tau \phi \right) - H(\tau) \right). \tag{4.8}$$

The constraint (3.6) has then to be imposed on the states at some initial time.

[4]The presence of two extra factors of ρ in the definition of $\mathcal{F}$, or rather the absence of these factors in $\mathcal{E}$, deserves an explanation. As explained above, these factors are needed in the vertex to ensure that the corresponding sites are occupied by solid lines. In contrast, in eq. (3.10), there is no need to introduce these factors, since the combination of fields $\phi^\dagger\phi$ at σ and σ' guarantees that the lines located at these sites are solid.

5. The variational approximation

The Hamiltonian developed in the last section is exact but it is also quite complicated. Clearly, to make progress, one has to resort to some approximation scheme. What we are trying to calculate is the structure of the ground state of the system, and for this purpose, the variational approach is the natural approximation scheme, although it is also possible to do an equivalent mean field calculation. In particular, as we have explained in the introduction, we are interested in phenomenon of the condensation of graphs on the world sheet, by which we mean the following: Consider the limit of a large but finite number of lines, that is

$$N_0 = p^+/a \tag{5.1}$$

is large but finite. Here, p^+ total + momentum flowing through the graph and a is the spacing between the lines. If in this limit the solid lines constitute a finite fraction of the total number of lines, we say that a condensate of solid lines has formed. Another equivalent way of defining the condensate is to use ρ (eq. (2.5)) as the order parameter. Consider the ground state expectation value of ρ,

$$\rho_0 = \langle \rho(\sigma, \tau) \rangle. \tag{5.2}$$

We will assume the ground state is invariant under the translations of σ and τ, so that ρ_0 does not depend on these variables. By its definition, ρ_0 measures the quantity we are interested in, namely, the probability of an average line in the ground state of the system being solid. In any fixed order of perturbation expansion, and in the limit of large N_0, ρ_0 is effectively zero, since the vast majority of the world sheet lines will be dotted. On the other hand, a finite ρ_0 means that the ground state is dominated by graphs whose order grow with N_0. We will find that, within our approximation scheme, ρ acquires a finite expectation value, signaling the formation of the condensate. In carrying out this calculation, we will also learn how to renormalize the model within this approximation, and we will compare it to the standard results from perturbation theory.

The ansatz for the ground state that will be used in the variational calculation is,

$$|s_v\rangle = \prod_\sigma \left(\int d\mathbf{q}\, A(\mathbf{q})\, \phi^\dagger(\sigma, \mathbf{q})\, \rho_-(\sigma) + B \right) |0\rangle, \tag{5.3}$$

where the product extends over all the sites and the vacuum state on the right is defined by (3.2). It easy to see that since A and B are σ independent, $|s_v\rangle$ is the direct product of identical states located at each site. It is therefore just about the simplest non-trivial ansatz for the ground state one can think of. A and B satisfy the normalization condition

$$\int d\mathbf{q}\, |A(\mathbf{q})|^2 + |B|^2 = 1.$$

In fact, each term in the above equation has a probability interpretation. From the definition of ρ_0, it follows that

$$\int d\mathbf{q}\, |A(\mathbf{q})|^2 = \rho_0 \tag{5.4}$$

is the probability of having a solid line at any site, and

$$|B|^2 = 1 - \rho_0 \tag{5.5}$$

is the probability of having a dotted line. The variational ansatz therefore represents a world sheet uniformly (independent of σ) populated by an arbitrary superposition of solid and dotted lines.

Following the standard variational principle, we will try to minimize the expectation value

$$\langle s_v|H|s_v\rangle$$

by setting its variation with respect to $A(\mathbf{q})$ and B equal to zero. We will take both A and B to be real, which can be done without any loss of generality, and set

$$B = \sqrt{1-\rho_0}.$$

Also, assuming that the ground state is rotationally invariant, A can only depend on the length of the vector $\mathbf{q}$. The normalization condition will be taken care of by defining

$$I(A,\rho_0,\lambda) = \langle s_v|H|s_v\rangle + \lambda\left(\int d\mathbf{q}\, A^2(\mathbf{q}) - \rho_0\right), \tag{5.6}$$

and varying I instead of $\langle s_v|H|s_v\rangle$. Here λ is a Lagrange multiplier.

Next, we need the expectation value of

$$H = H_0 + H_I$$

in the variational state. After a straightforward calculation, we have,

$$\langle s_v|H_0|s_v\rangle = \sum_{\sigma'>\sigma} \frac{\mathcal{E}(\sigma,\sigma')}{\sigma'-\sigma} \int d\mathbf{q}\left(\mathbf{q}^2 + \frac{1}{2}m^2\right) A^2(\mathbf{q}) \int d\mathbf{q}'\, A^2(\mathbf{q}'), \tag{5.7}$$

and,

$$\langle s_v|H_I|s_v\rangle = 2g\,B \sum_{\sigma} \mathcal{V}(\sigma) \int d\mathbf{q}\, A(\mathbf{q}). \tag{5.8}$$

We note that in deriving eq. (5.7), one has to expand the expression $(\mathbf{q}-\mathbf{q}')^2$ in eq. (3.10). The cross term $\mathbf{q}\cdot\mathbf{q}'$ in this expansion does not contribute because of the rotation invariance of the A's.

The indicated sums over σ and σ' are easily done, after $\rho(\sigma)$ in eqs. (3.9) and (4.5) is replaced by ρ_0, a σ independent constant. We have,

$$\sum_{\sigma'>\sigma} \frac{\mathcal{E}(\sigma,\sigma')}{\sigma'-\sigma} = \sum_{\sigma}\sum_{n=0}^{\infty} \frac{(1-\rho_0)^n}{a(n+1)} = -\frac{p^+}{a}\,\frac{\ln(\rho_0)}{a\,(1-\rho_0)}, \tag{5.9}$$

and therefore,

$$\langle s_v|H_0|s_v\rangle = \frac{p^+}{a}\left(-\frac{\rho_0\,\ln(\rho_0)}{2a(1-\rho_0)} \int d\mathbf{q}\,(2\mathbf{q}^2+m^2)A^2(\mathbf{q})\right), \tag{5.10}$$

where eq. (5.4) was used.

After setting $\rho = \rho_0$, $\mathcal{V}$ becomes σ independent, but it still depends on ρ_0. We are unable to express this dependence in terms of elementary functions, so instead, we define,

$$W(\rho_0) = \sum_{n_1=0}^{\infty} \sum_{n_2=0}^{\infty} \frac{(1-\rho_0)^{n_1+n_2+1}}{\sqrt{(n_1+1)(n_2+1)(n_1+n_2+2)}}, \tag{5.11}$$

and write,

$$\langle s_v | H_I | s_v \rangle = 2\,\frac{p^+}{a}\,\frac{g}{\sqrt{8a^3}}\,\sqrt{1-\rho_0}\,W(\rho_0)\int d\mathbf{q}\,A(\mathbf{q}). \tag{5.12}$$

In deriving eqs. (5.9) and (5.11), we have assumed that the upper limit of the sum over the σ's can be extended to to infinity, whereas in reality, there is a cutoff at $\sigma = p^+$. For example, W has a spurious singularity as $\rho_0 \to 0$,

$$W(\rho_0) \to \pi^{3/2}\,(\rho_0)^{-1/2}, \tag{5.13}$$

which would be absent if the cutoff is imposed. Thus, the neglect of this cutoff makes a difference only for small values of ρ_0. Although it is not difficult to take care of the cutoff, the resulting formulas become complicated. In the interests of simplicity, we will work with the expressions derived above, keeping in mind the restriction that they are not reliable for small values of ρ_0.

Putting together eqs. (5.6), (5.10) and (5.12), I given by

$$\begin{aligned} I = &-\frac{p^+\,\ln(\rho_0)}{2a^2(1-\rho_0)}\int d\mathbf{q}\,(2\mathbf{q}^2+m_0^2)\,A^2(\mathbf{q}) \\ &+\frac{2p^+\,g_0}{\sqrt{8a^5}}\,\sqrt{1-\rho_0}\,W(\rho_0)\int d\mathbf{q}\,A(\mathbf{q}) + \lambda\left(\int d\mathbf{q}\,A^2(\mathbf{q}) - \rho_0\right). \end{aligned} \tag{5.14}$$

The first variational equation,

$$\frac{\delta I}{\delta A(\mathbf{q})} = 0, \tag{5.15}$$

determines the functional dependence of A on $\mathbf{q}$:

$$A(\mathbf{q}) = -\frac{g_0}{\sqrt{2a}}\,\frac{\sqrt{1-\rho_0}\,W(\rho_0)}{\tilde{\lambda} + F(\rho_0)(2\mathbf{q}^2+m_0^2)}, \tag{5.16}$$

where we have defined,

$$\tilde{\lambda} = \frac{2\lambda\,a^2}{p^+},\quad F(\rho_0) = -\frac{\rho_0\,\ln(\rho_0)}{1-\rho_0}. \tag{5.17}$$

In anticipation of renormalization, when one has to distinguish between bare and renormalized constants, m and g were replaced by m_0 and g_0.

From the above equation, it is easy to see that A has the form of a free light cone propagator. In fact, setting,

$$A(\mathbf{q}) = \frac{const.}{\mathbf{q}^2+m_r^2},$$

where,

$$m_r^2 = \frac{m_0^2}{2} + \frac{\tilde{\lambda}}{2F(\rho_0)}, \tag{5.18}$$

we can identify m_r with the renormalized mass.

Next, varying I with respect to λ, reproduces the normalization condition (5.4). We will see that the resulting equation fixes the value of ρ_0, the parameter of interest. Replacing A by (5.16), the integral involving A^2 can be explicitly evaluated. At this point, the dimension of the transverse space, which has been so far left arbitrary, has to be specified. The critical dimension of the ϕ^3 theory is six, corresponding to $D = 4$, accordingly, in what follows, we will take $D = 4$, although we could also have studied lower dimensions. The integral in question is then logarithmically divergent, and it will be regulated by cutting it off at $|\mathbf{q}| = \Lambda$. From now on, we will focus on the cutoff dependent terms in the equations, and generally neglecting the finite corrections. We will see that the finite terms can be absorbed into the definition of the renormalized parameters.

Evaluating the logarithmic term in the integral

$$\int d^4q A^2(\mathbf{q}) \to 2\pi^2 \int_0^\Lambda dq\, q^3 A^2(\mathbf{q}) \approx \frac{g_0^2\,\pi^2\,(1-\rho_0)\,W^2(\rho_0)}{4\,a\,F^2(\rho_0)}\,\ln\left(\frac{\Lambda}{\mu}\right), \tag{5.19}$$

the normalization condition reads,

$$\rho_0 = \frac{g_0^2\,\pi^2\,(1-\rho_0)\,W^2(\rho_0)}{4\,a\,F^2(\rho_0)}\,\ln\left(\frac{\Lambda}{\mu}\right) + finite\,terms. \tag{5.20}$$

Here μ is mass parameter whose value depends on the finite terms discussed above. Although these terms can be evaluated, in the subsequent development, we will mainly be interested in the cutoff dependence and renormalization. In fact, if so desired, one can completely absorb the finite terms into the definition of μ.

From its definition as a probability, we know that ρ_0 lies between zero and one and therefore cannot depend on the cutoff Λ. This can be arranged by defining the renormalized coupling constant by

$$g_r^2 = g_0^2\,\ln\left(\frac{\Lambda}{\mu}\right). \tag{5.21}$$

This equation is consistent with the one loop renormalization group equation, leading to asymptotic freedom, and in agreement with the fact that ϕ^3 theory is known to be asymptotically free in six dimensions.

At this point, a natural question arises: How is it that in a phase dominated by graphs of infinite order, the ultraviolet divergences agree with those deduced from perturbation theory? This is somewhat of a surprize, and at least a partial explanation is the following. The calculation presented here amounts to expanding the fields ϕ and $\phi^\dagger$ about the classical background $A(\mathbf{q})$, given by eq. (5.16). In this sense, it is very similar to the usual field theory calculations in the presence of a classical background, such as expanding about an instanton in non-abelian gauge theories. In these calculations with a classical background, the ultraviolet divergences are the same as in perturbation theory, and the standard explanation is that the "soft" background does not change the leading short

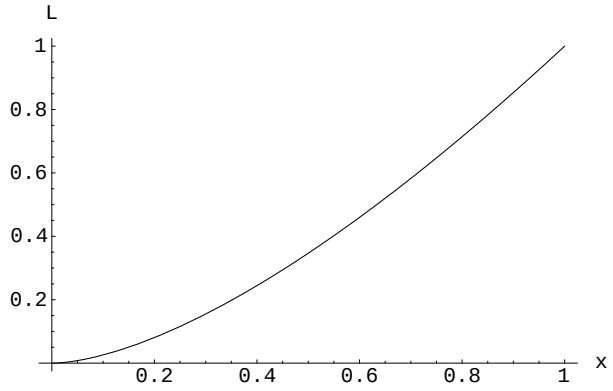

Figure 6: The Function L(x)

distance singularities. Presently, work is in progress to reformulate the variational calculation as a systematic expansion around the classical background. Such a reformulation, if successful, would substantiate the explanation presented above.

Eq. (5.20) can be rewritten in terms of the renormalized coupling constant as

$$\rho_0 = \frac{\tilde{g}^2\,(1-\rho_0)\,W^2(\rho_0)}{F^2(\rho_0)}, \tag{5.22}$$

where, for convenience, we have defined,

$$\tilde{g}^2 = \frac{g_r^2\,\pi^2}{4\,a}.$$

This is the equation that determines ρ_0. The question is then whether this equation has a solution for $0 \leq \rho_0 \leq 1$. To further simplify matters, we take the square root of (5.22) and define,

$$\rho_0 = x, \;\; x\,F(x) = L(x), \;\; \sqrt{x(1-x)}\,W(x) = Z(x),$$

and rewrite it as,

$$L(x) = |\tilde{g}|\,Z(x). \tag{5.23}$$

As shown in figure 6, $F(x)$ is zero at $x = 0$, and steadily increases to $F = 1$ at $x = 1$. On the other hand, Z is equal to $\pi^{3/2}$ at $x = 0$ (see eq. (5.13)), and steadily goes down to $Z = 0$ at $x = 1$. Z is plotted for $x > 0.1$ in figure 7. Clearly, if $\tilde{g} \neq 0$, the two curves must intersect for some $0 < x < 1$, as shown in figure 8 for $\tilde{g} = 1$. This shows that $\rho_0 = x \neq 0$, and therefore a condensate forms for non-zero renormalized coupling. As $\tilde{g} \to 0$, the intersection point approaches $x = 0$, and explained in the paragraph after eq. (5.12), the expressions for L and Z become unreliable. In any case, as the coupling tends to zero, we expect perturbation theory to take over and the condensate to dissolve.

The third and the final variational equation, combined with eq. (5.18), enables one to express the bare mass and the parameter $\tilde{\lambda}$ in terms of m_r and g_r. It is gotten by varying

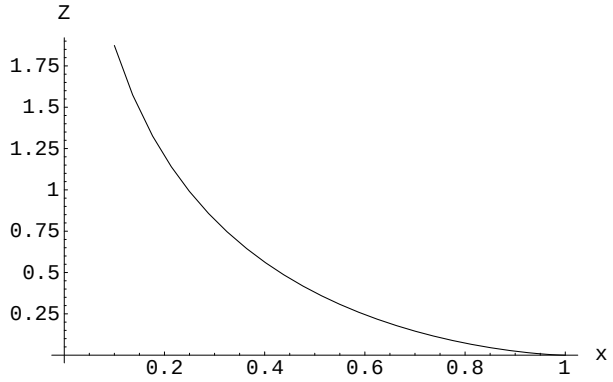

Figure 7: The Function Z(x)

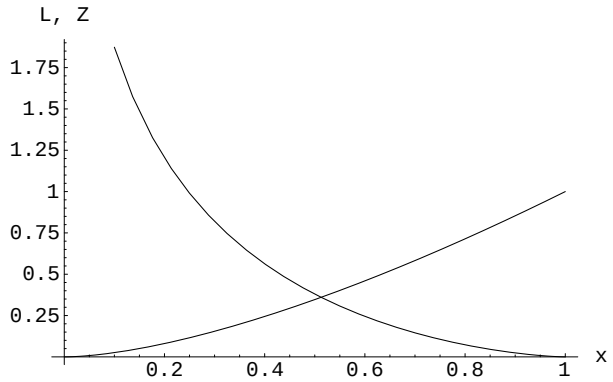

Figure 8: The Combined Plot Of L(x) And Z(x)

I with respect to ρ_0:

$$\frac{2a^2}{p^+}\frac{\partial I}{\partial \rho_0} = \sqrt{\frac{2}{a}}\, g_0 \left(\sqrt{1-\rho_0}\, W(\rho_0)\right)' \int d\mathbf{q}\, A(\mathbf{q}) + F'(\rho_0) \int d\mathbf{q}\, \left(2\mathbf{q}^2 + m_0^2\right)\, A^2(\mathbf{q}) - \tilde{\lambda} = 0, \tag{5.24}$$

where the prime indicates the derivative with respect to ρ_0. Substituting eq. (5.16) for A, this time we encounter quadratic divergences at $D = 4$. Introducing the cutoff Λ as in eq. (5.19), and keeping only the leading quadratic divergence, gives the result,

$$\rho_0\, F'\, m_0^2 - \tilde{\lambda} = \frac{g_0^2\, \pi^2\, \Lambda^2}{4a\, F^2} \left(F\, \left((1-\rho_0)\, W^2\right)' - (1-\rho_0)\, F'\, W^2\right) + finite\, terms. \tag{5.25}$$

One can now solve the two linear equations (5.18) and (5.25) for m_0^2 and $\tilde{\lambda}$, and express them in terms of g_r (replacing g_0 by g_r through (5.21)), m_r and the cutoff Λ. The bare mass and coupling are thus expressed in terms of the renormalized mass and coupling and the cutoff; therefore, at least in this approximation, the model is successfully renormalized.

Part of the the calculation presented above has obvious overlap with perturbation theory: For example, the identification of $A(\mathbf{q})$ with the free propagator, the cutoff dependence

of bare parameters and the relation between bare and renormalized couplings (asymptotic freedom) all parallel standard perturbative results. On the other hand, our variational calculation goes beyond perturbation theory. For example, the functions F and W have no obvious perturbative interpretation. In particular, we have argued earlier that ρ_0 is zero in any finite order of perturbation, whereas the eq. (5.22) has a solution $\rho_0 \neq 0$ for $g_r \neq 0$. The formation of a condensate is therefore clearly a non-perturbative phenomenon.

A somewhat surprising feature of the variational ansatz (5.3) is that it is not an eigenstate of the total momentum operator

$$\mathbf{P} = \sum_{\sigma} \int d\mathbf{q}\, \mathbf{q}\, \phi^{\dagger}(\sigma, \mathbf{q})\, \phi(\sigma, \mathbf{q}). \tag{5.26}$$

Only the expectation value of $\mathbf{P}$ is well defined and it is zero:

$$\langle s_v | \mathbf{P} | s_v \rangle = 0. \tag{5.27}$$

This follows from the rotation invariance of the function $A(\mathbf{q})$. Of course, this does not mean that conservation of momentum is violated. The real ground state is an eigenstate of momentum with eigenvalue zero. What this really means is that the trial ground state we are using is a superposition of states with different momenta, with only the average momentum fixed at zero. States of this type are commonly used in statistical mechanics to construct the grand canonical ensemble; an ensemble of states with varying particle number is a typical example. We note that, since the boundary conditions at the initial and final times were left free, world sheet configurations of arbitrary total momenta are allowed. Of course, we could constrain the total momentum of the trial state to be zero by, for example, setting the momentum at a particular site to be minus the sum of the momenta at the other sites. However, this would complicate the variational calculation considerably, and in the limit of large number of sites, it would probably not change the final outcome significantly. In any case, whether a trial wave function approximates the real one reasonably well is always an open question.

Finally, a few words about the decompactification limit $a \to 0$ are in order. At the beginning, N_0 (eq. (5.1)) was specified to be large but finite. It had to be large to be able to define a condensate in the first place, and it had to be finite to avoid possible infrared singularities. The question arises: Are there singularities in the limit $a \to 0$? Consider the equations we have derived in this section, for example, equations (5.22) and (5.25). Expressed in terms $\tilde{g}$, these equations do not depend on a anymore. So a simple redefinition of the coupling constant eliminates possible singulaties. Of course, this is not the whole story: Higher order corrections to our approximation may turn to be singular in the decompactified model. We hope to study this problem in the future.

6. Conclusions

The present work is a fresh approach to the old problem of the summation of planar graphs [9, 10]. Although it has some overlap with the earlier work by Thorn and the present author [1 – 4], especially with reference [4], it is essentially a fresh start. The main

difference with the earlier work is that it is based on second quantization rather than first quantization. Just as in the usual second quantized field theory, the Hamiltonian is expressed in terms of creation and annihilation operators, except that these operators, instead of particles, create and annihilate boundaries on the world sheet. With the help of a simple variational ansatz, we were able to investigate the structure of the ground state. In particular, we were able to show that the ground state was a condensate of boundaries (solid lines). This calculation was carried out in six dimensional space-time, which is the critical dimension of the ϕ^3 theory. The ultraviolet divergences encountered in the course of the variational calculation are completely consistent with standard perturbation results, and they can be renormalized in the usual fashion.

We hope to follow up on the present work along various directions. For example, either using a variational or a mean field method, it should be possible to go beyond the ground state of the model and investigate the whole spectrum of excited states. This should give us information about possible string formation, which we have not discussed here. Another interesting future project is to study the limit of continuum world sheet by decompactifying the model. In this limit, one expects a simpler local field theory to emerge from the non-local model presented here. Finally, building on the earlier work [11, 12], we hope to incorporate a physical theory such as QCD into the framework developed here.

Acknowledgments

This work was supported by the Director, Office of Science, Office of High Energy Physics, of the U.S. Department of Energy under Contract DE-AC02-05CH11231.

References

[1] K. Bardakci and C.B. Thorn, *A worldsheet description of large-N_c quantum field theory*, *Nucl. Phys.* **B 626** (2002) 287 [hep-th/0110301].

[2] K. Bardakci and C.B. Thorn, *A mean field approximation to the world sheet model of planar ϕ^3 field theory*, *Nucl. Phys.* **B 652** (2003) 196 [hep-th/0206205].

[3] K. Bardakci, *Further results about field theory on the world sheet and string formation*, *Nucl. Phys.* **B 715** (2005) 141 [hep-th/0501107].

[4] K. Bardakci, *Planar graphs on the world sheet: the hamiltonian approach*, *JHEP* **07** (2008) 057 [arXiv:0804.1329].

[5] G. 't Hooft, *A planar diagram theory for strong interactions*, *Nucl. Phys.* **B 72** (1974) 461.

[6] K. Bardakci, *Self consistent field method for planar ϕ^3 theory*, *Nucl. Phys.* **B 677** (2004) 354 [hep-th/0308197].

[7] T. Banks, W. Fischler, S.H. Shenker and L. Susskind, *M theory as a matrix model: a conjecture*, *Phys. Rev.* **D 55** (1997) 5112 [hep-th/9610043].

[8] L. Susskind, *Another conjecture about M(atrix) theory*, hep-th/9704080.

[9] H.B. Nielsen and P. Olesen, *A parton view on dual amplitudes*, *Phys. Lett.* **B 32** (1970) 203.

[10] B. Sakita and M.A. Virasoro, *Dynamical model of dual amplitudes*, *Phys. Rev. Lett.* **24** (1970) 1146.

[11] S. Gudmundsson, C.B. Thorn and T.A. Tran, *BT worldsheet for supersymmetric gauge theories*, *Nucl. Phys.* **B 649** (2003) 3 [hep-th/0209102].

[12] C.B. Thorn and T.A. Tran, *The fishnet as anti-ferromagnetic phase of worldsheet Ising spins*, *Nucl. Phys.* **B 677** (2004) 289 [hep-th/0307203].

JHEP10(2008)056